



Contents lists available at www.sciencedirect.com

Journal of the European Ceramic Society

journal homepage: www.elsevier.com/locate/jeurceramsoc



Effect of metallization on the strength and fracture behaviour of functional co-fired multilayer ceramics

M. Gruber^a, P. Supancic^{a,b}, F. Aldrian^c, R. Bermejo^{a,*}

^a Institut für Struktur – und Funktionskeramik, Montanuniversität Leoben, Austria

^b Materials Center Leoben Forschung GmbH, Leoben, Austria

^c EPCOS OHG, Deutschlandsberg, Austria

ARTICLE INFO

Article history:

Received 22 December 2016

Received in revised form 7 February 2017

Accepted 8 February 2017

Available online xxx

Keywords:

Functional ceramic components

Miniaturized mechanical testing

Strength distribution

Damage

Fractography

ABSTRACT

Functional components are commonly fabricated combining a ceramic substrate with external and/or internal metallization. Different layers are printed and fired onto the ceramic part to provide the component with a functionality. As a result of the combination of materials with different coefficients of thermal expansion, internal stresses during the fabrication steps may lead to cracks and/or reduce the strength. In this work, several architectures combining metal and glass layers on the surface of ZnO substrates were analyzed to identify critical fabrication steps in functional co-fired multilayer ceramics. Three-point bending tests were performed on samples taken after different process steps. Experimental results showed a strong effect of the layered architecture on the strength distributions: details of geometrical designs can have a dramatic impact on the strength. Fractographic analyses and *ex-situ* Focused Ion Beam experiments in pre-loaded samples were the key to assess the location of failure and predict critical configurations.

© 2017 Elsevier Ltd. All rights reserved.

1. Introduction

In many applications for microelectronics it is necessary to combine different materials (ceramic, metals and polymers) that can bring new functionality to components, creating so-called hybrid planar systems. Functional components such as multilayer varistors (MLV), multilayer piezoelectric actuators (MPA), multilayer ceramic capacitors (MLCC), Low Temperature Co-fired Ceramics (LTCC) and semiconductors, among others, are examples of combination of a ceramic-based (or silicon based) substrate with internal electrodes as well as surface features (e.g. metallization, contacting pads, cylindrical vias, etc.) However, it entails a number of multidisciplinary challenges which have to be solved (e.g. geometrical tolerances, fabrication of internal structures, co-sintering of different materials, development of internal stresses, etc.) In this regard, tape casting technology has enabled the fabrication of such hybrid devices based on a “multilayer architectural design”, with high degree of dimensional accuracy [1,2]. Some examples of such advanced engineering systems are (i) planar Solid Oxide Fuel Cells (SOFC), (ii) stacked piezo-actuators and sensor devices, and (iii) conducting plates for wireless communications. Typical

components are based on low temperature co-fired ceramics substrates (e.g. alumina-glass composites, ZnO), which enable the co-sintering of (low melting point) glass ceramics with high electrical conductivity materials (e.g. silver, gold, galvanized nickel) [3]. In the co-sintering process, different layers are printed and/or sintered (e.g. up to 900 °C) onto the ceramic substrate according to the component design. In any case, the fabrication of components having two or more different materials can be a challenge from the structural viewpoint. The different thermal expansion coefficients and elastic properties of the combined materials can generate significant “residual stresses” in some of the parts (e.g. in the ceramic layers), which may induce cracks that truncate the electrical performance of the component [4,5]. While compressive residual stresses can be beneficial in strengthening the material (e.g. ion exchange process as used in Gorilla® glass [6,7]), tensile residual stresses may lead to the initiation and/or propagation of cracks (e.g. surface cracks) from starting defects, even before service loading conditions [8]. In addition, although some of these tensile residual stresses may relax due to plastic deformation of metallic materials, stress concentrations generated in material junctions or terminations (imposed by geometrical constraints) may lead to failure during fabrication or in service.

In a previous work the fracture behavior of a co-fired multilayer structure based on ZnO ceramic substrate was investigated [9]. Two architectures were analyzed, holding a slightly different combina-

* Corresponding author.

E-mail address: raul.bermejo@unileoben.ac.at (R. Bermejo).

tion of metal and glass layers onto the substrate material. In one case, a significant different strength distribution was found, as compared to bulk ZnO material. A FE analysis simulating the residual stress distribution during the fabrication process showed relatively high stress concentration in the junction between metal and glass layers [9]. Such location was found to be the fracture origin in both configurations (i.e. crack initiation). A fracture mechanics analysis showed a preferred angle of crack propagation, being closed to the metal-glass interface. Nevertheless, based on those results, the difference in strength between both configurations remained unclear. This previous work demonstrated that the different steps during the fabrication of the multilayer architecture may have played a role on the final behavior of the structure.

In this work the effect of metallization steps and layered architecture on the fracture behaviour of ceramic-based functional multilayer components has been experimentally assessed. Different configurations of metal and glass layers attached onto the surface step by step were analyzed. Mechanical testing using three-point bending was performed on samples taken after different process steps and compared to the strength distribution of the bulk substrate material. Strength results were interpreted according to Weibull statistics. In order to identify the failure origin in the different architectures, fractographic analyses were performed on broken samples. In addition, Focused-Ion-Beam (FIB) analyses were carried out on preloaded (pre-damage) samples to understand the onset and propagation of cracks during mechanical loading.

2. Materials and architectures

Fig. 1 schematically shows the typical build-up of the functional multilayer architecture (thereafter referred to as FMA) of study. The fabrication process is described in detail in Ref. [9]. It consists of a ZnO ceramic substrate (green), two silver metallization layers (light blue), a glass layer in between (blue) and a nickel (Ni) galvanic coating (orange). The typical dimensions of such FMA components are given in Fig. 1a. A detail of the cross-section of the component is shown in Fig. 1b. It is worth pointing out that the overlapping of the two metallization layers (i.e. M1 and M2) can be done following two distinct configurations. In configuration 1 (referred to as Conf. 1) the area covered by the metallization 1 (M1) is larger than that of metallization 2 (M2), see Fig. 1c. In configuration 2 (named as Conf. 2) the area metallization 2 (M2) is the one covering a larger area, see Fig. 1d. For both configurations, after the co-firing of the ZnO substrate with internal electrodes and vias, the FMA is produced following these process steps: (i) first metallization of silver (M1) onto the ZnO substrate, (ii) printing of a glass layer, (iii) second metallization of silver (M2) onto the top of M1 and the glass layer,

and (iv) galvanization of the electroless nickel ($\sim 4 \mu\text{m}$ layer) on the metallization M2 followed by a very thin gold layer ($\sim 60 \text{ nm}$), see top (orange) layer in Fig. 1. For illustrative purposes, a schematic of the different steps for both configurations along with a top view of the structures are represented in Fig. 2. It should be noticed that both configurations were manufactured in the same manner. The only difference between these two configurations is the size ratio between metallization M1 and M2, with $M1/M2 > 1$ for Conf. 1 and $M1/M2 < 1$ for Conf. 2. No other influences of the processing are to be expected. The cross-section in Fig. 1b provides a closer look into the structure and shows the differences in geometry of the metal layers from the side view.

3. Mechanical characterization

3.1. Testing samples

Bending bars were fabricated for the mechanical testing, containing equally spaced distributed FMA components corresponding to Conf. 1 and Conf. 2, see Fig. 3a and b, respectively. For comparison, bulk bending bars were also tested (Fig. 3c). Typical dimensions were ($l \times b \times t$) $25 \text{ mm} \times 3.8 \text{ mm} \times \sim 0.25 \text{ mm}$, with l , b and t being the length, width and thickness of the specimen, respectively. Details on specimens preparation can be found in [9].

3.2. Strength evaluation

The bending tests were performed according to the ASTM C1161 standard [10] using a three-point bend (3PB) fixture, with an outer span S_0 of 20 mm. Tests were conducted in ambient conditions (25°C , 15% relative humidity) under displacement control with a load cell of 200 N at a rate of 5 mm/min using a universal testing machine (Zwick Z1010, Zwick/Roell, Ulm, Germany). The maximum stress in the specimen during the bending test (failure stress), σ_f , was calculated for each bar following the expression [10]:

$$\sigma_f = \frac{3}{2} \frac{PS_0}{bt^2} \quad (1)$$

where P is the fracture load. The thickness t was considered to be the substrate thickness for the bulk samples, and the thickness of substrate plus glass layer for the FMA samples.

3.3. Fractographic analyses

The light microscope images (LIMI) were made on an optical microscope (BX50, Olympus, Tokyo, Japan). The scanning electron microscope (SEM) images and focused ion beam (FIB) cuts were performed in a SEM (Auriga, Zeiss, Germany) equipped with a FIB

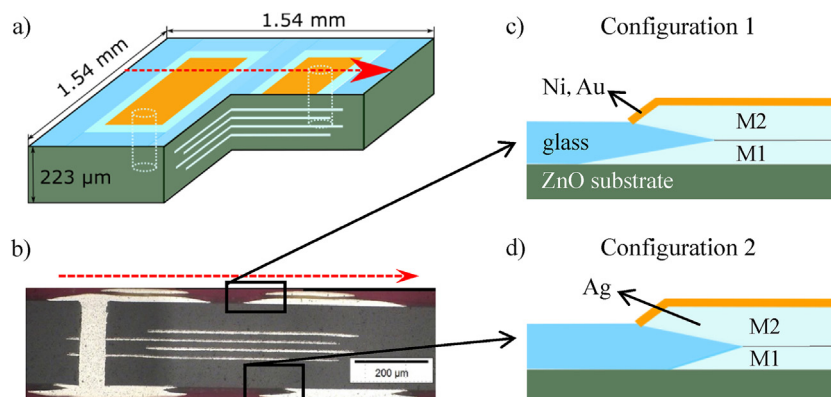


Fig. 1. (a) 3D schematic of the FMA component, (b) Cross-section showing the top and bottom architecture of the FMA (c) Metallization configuration 1 (Conf. 1), (d) Metallization configuration 2 (Conf. 2). (For interpretation of the references to colour in the text, the reader is referred to the web version of this article.)

Download English Version:

<https://daneshyari.com/en/article/5440574>

Download Persian Version:

<https://daneshyari.com/article/5440574>

[Daneshyari.com](https://daneshyari.com)